

## Electronic Supplementary Information

### **Fe<sub>3</sub>O<sub>4</sub> Embedded ZnO Nanocomposites for Removal of Toxic Metal Ions, Organic Dyes and Bacterial Pathogen**

*Sarika Singh<sup>a</sup>, K. C. Barick<sup>b</sup>, and D. Bahadur<sup>a,\*</sup>*

<sup>a</sup> Dept. of Metallurgical Engineering and Materials Science,  
Indian Institute of Technology Bombay, Mumbai – 400076, India

<sup>b</sup> Chemistry Division, Bhabha Atomic Research Centre, Mumbai – 400085, India

\* Corresponding author:- Tel.: +91 22 2576 7632, Fax: +91 22 2572 3480, E-mail: dhiren@iitb.ac.in

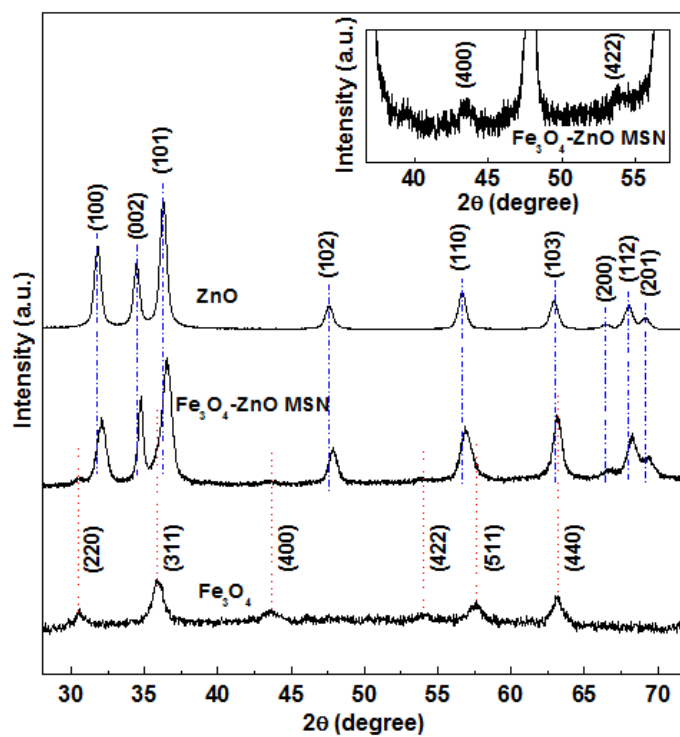


Fig. S1. XRD patterns of the  $\text{Fe}_3\text{O}_4$ , ZnO, and  $\text{Fe}_3\text{O}_4$ -ZnO MSN. Inset shows the expanded XRD pattern of  $\text{Fe}_3\text{O}_4$ -ZnO MSN revealing (400) and (422) planes of  $\text{Fe}_3\text{O}_4$ .

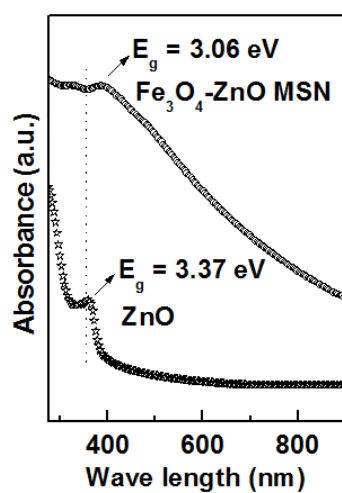


Fig. S2. UV-visible absorption spectra of ZnO and  $\text{Fe}_3\text{O}_4$ -ZnO MSN.

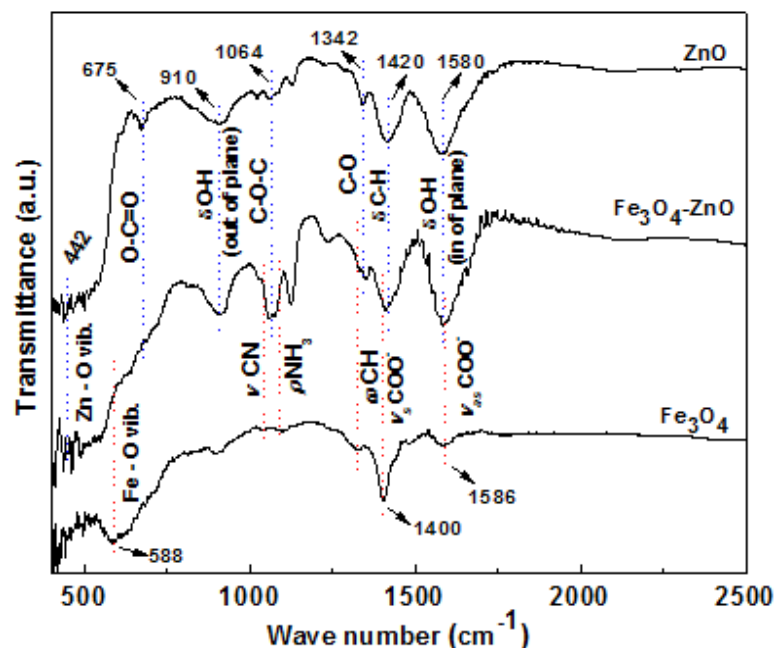


Fig. S3. FTIR spectra of ZnO, Fe<sub>3</sub>O<sub>4</sub> and Fe<sub>3</sub>O<sub>4</sub>-ZnO MSN with their corresponding peak assignments. The bands appeared at 1580 and 910 cm<sup>-1</sup> in FTIR spectra of ZnO are due to in and out of plane of O-H stretching vibration, respectively. The absorption bands appeared at 675, 1064 and 1420 cm<sup>-1</sup> in ZnO can be ascribed to O-C=O vibration, C-O-C vibration and C-H bending modes, respectively. The peak appeared at 422 cm<sup>-1</sup> and 588 cm<sup>-1</sup> corresponds to vibrational modes of Zn-O and Fe-O, respectively. The band observed at 1400 and 1586 cm<sup>-1</sup> in FTIR spectra of Fe<sub>3</sub>O<sub>4</sub> corresponds to symmetric and asymmetric stretching modes of COO<sup>-</sup> group. It has been observed that the important characteristic vibrational bands of Fe<sub>3</sub>O<sub>4</sub> and ZnO are appeared in the FTIR spectra of Fe<sub>3</sub>O<sub>4</sub>-ZnO MSN with a slight shifting and/ or broadening band). The results clearly suggest the presence of Fe<sub>3</sub>O<sub>4</sub> and ZnO in Fe<sub>3</sub>O<sub>4</sub>-ZnO MSN.

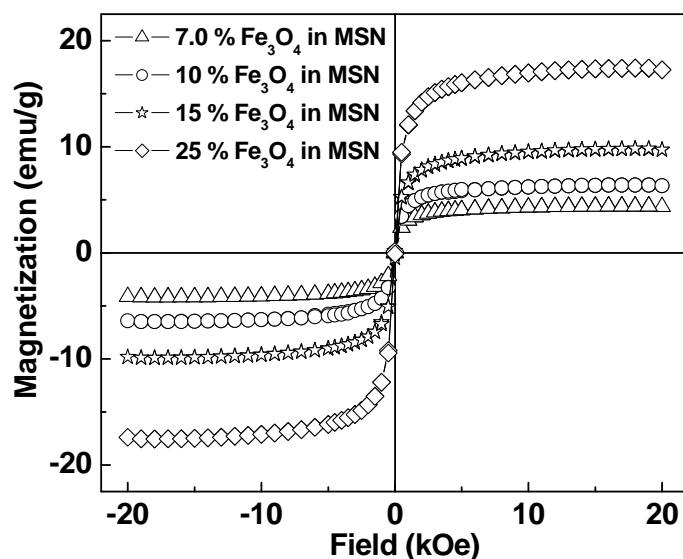


Fig. S4. Room temperature field dependence of magnetization ( $M$  vs.  $H$ ) plot of  $\text{Fe}_3\text{O}_4$ -ZnO MSN containing different wt. % of  $\text{Fe}_3\text{O}_4$  nanoparticles.

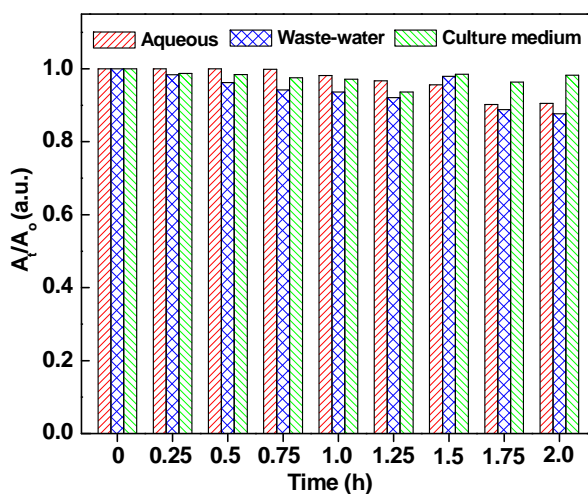


Fig. S5. Normalized UV absorbance ( $A_t/A_0$ ) vs. time plot of  $\text{Fe}_3\text{O}_4$  - ZnO MSN (1.0 mg/ml) at wavelength of 370 nm in aqueous, waste-water and culture media ( $A_t$  = absorbance at time 't' and  $A_0$  = absorbance at  $t_0$ ). The insignificant change in absorbance of nanocomposite suspensions in aqueous, waste-water and bacterial culture media (1.0 mg/ml) indicates their good colloidal stability. Furthermore, the light scattering intensity and polydispersity index of MSN suspensions hardly varies with time (as observed from DLS measurements) revealing their excellent colloidal stability.

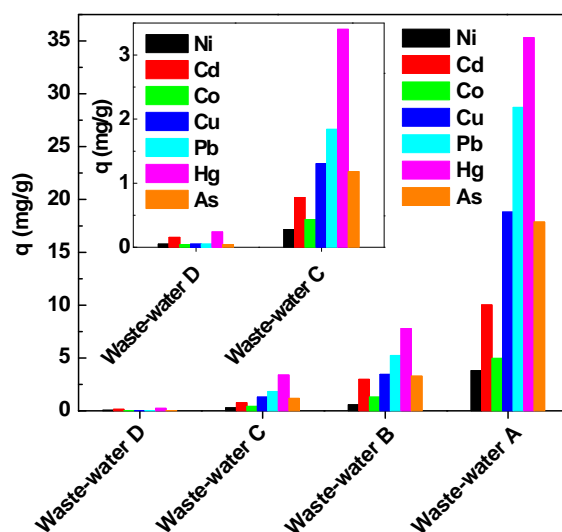


Fig. S6. The equilibrium adsorbed concentration,  $q$  (mg/g) of metal ions obtained after treating different waste-water with 50 mg of  $\text{Fe}_3\text{O}_4$ -ZnO MSN. Inset shows the results for waste-water C and D in expanded scale.

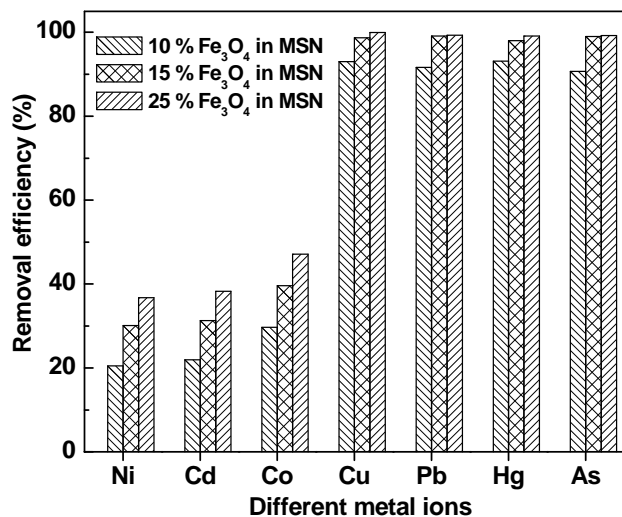


Fig. S7. Removal efficiency of metal ions by 50 mg of  $\text{Fe}_3\text{O}_4$ -ZnO MSN having 10, 15 and 25 wt. % of  $\text{Fe}_3\text{O}_4$  (MSN prepared with different amounts of  $\text{Fe}_3\text{O}_4$  nanoparticles).

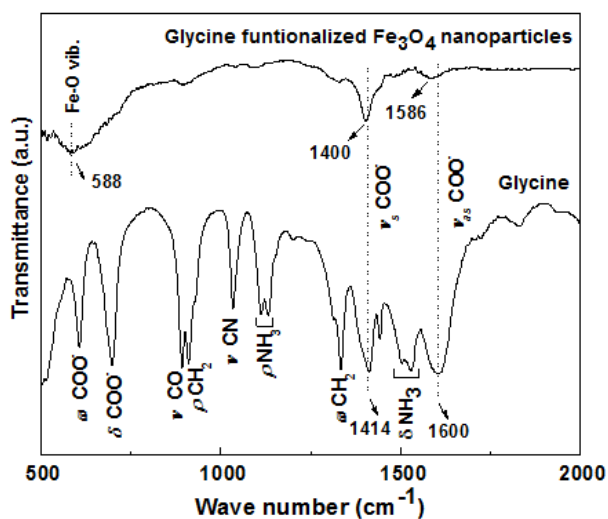


Fig. S8. FTIR spectra of glycine and glycine functionalized Fe<sub>3</sub>O<sub>4</sub> nanoparticles with their corresponding peak assignments (Most of the vibrational modes corresponding to pure glycine are observed in FTIR spectrum of glycine functionalized Fe<sub>3</sub>O<sub>4</sub> nanoparticles. The shifting of symmetric (ν<sub>s</sub>) and asymmetric (ν<sub>as</sub>) stretching modes of COO<sup>-</sup> group from 1414 to 1400 cm<sup>-1</sup> and 1600 to 1586 cm<sup>-1</sup>, respectively upon functionalization of Fe<sub>3</sub>O<sub>4</sub> clearly suggest the chemisorptions of glycine onto the Fe<sub>3</sub>O<sub>4</sub> through carboxylate group, leaving freely exposed amine groups).

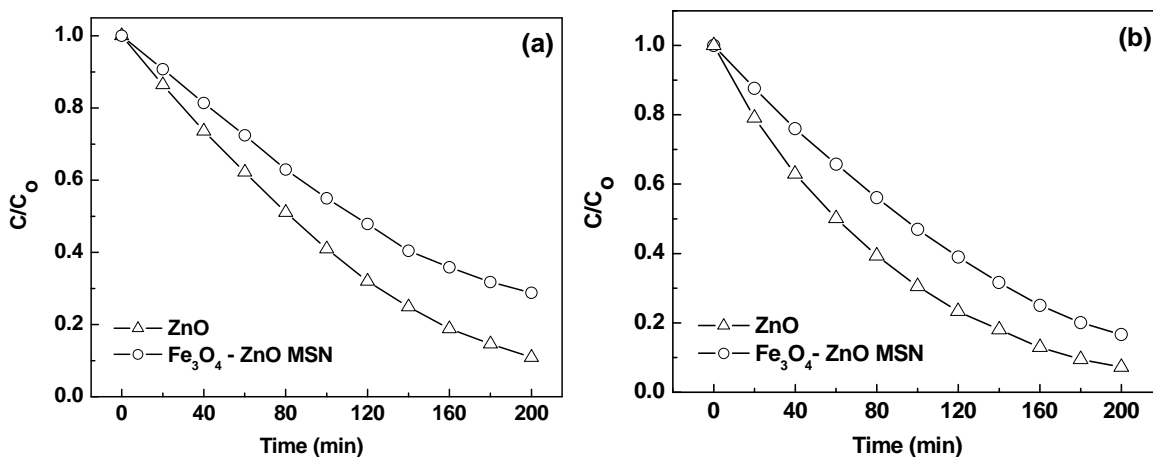


Fig. S9. Photodegradation of (a) MO and (b) RhB in the presence of Fe<sub>3</sub>O<sub>4</sub>-ZnO MSN under UV irradiation.

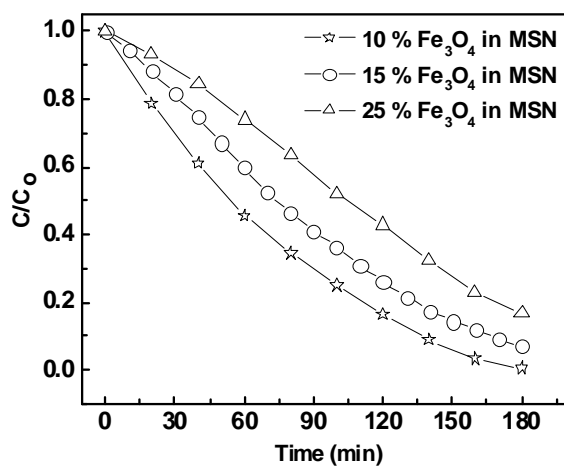


Fig. S10. Photodegradation of MB under UV irradiation in presence of Fe<sub>3</sub>O<sub>4</sub>-ZnO MSN having 10, 15 and 25 wt. % of Fe<sub>3</sub>O<sub>4</sub> (MSN prepared with different amount of Fe<sub>3</sub>O<sub>4</sub> nanoparticles).

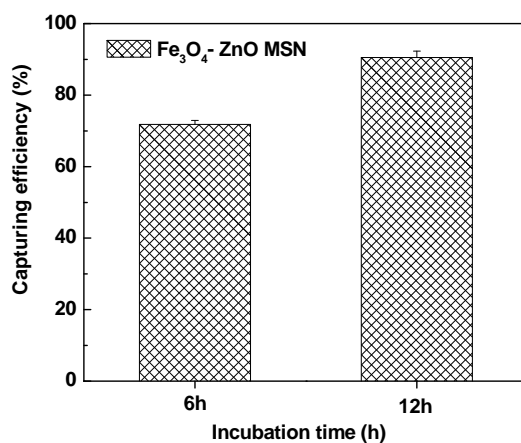


Fig. S11. Capture efficiency of *S. aureus* by 0.4 mg/ml of Fe<sub>3</sub>O<sub>4</sub>-ZnO MSN at different incubation time.